Published in final edited form as:
Proteomics. 2008 May ; 8(9): 1933–1944. doi:10.1002/pmic.200700859.

Proteomic Changes in Rat Thyroarytenoid Muscle Induced by Botulinum Neurotoxin Injection

Nathan V. Welham[1], **Gerard Marriott**[2], **Ichiro Tateya**[3], and **Diane M. Bless**[1]

1*Division of Otolaryngology-Head and Neck Surgery, Department of Surgery, University of Wisconsin School of Medicine and Public Health, Madison, WI, USA.*

2*Department of Physiology, University of Wisconsin School of Medicine and Public Health, Madison, WI, USA.*

3*Department of Otolaryngology-Head and Neck Surgery, Kyoto Katsura Hospital, Kyoto, Japan*

Abstract

Botulinum neurotoxin (BoNT) injection into the thyroarytenoid (TA) muscle is a commonly performed medical intervention for adductor spasmodic dysphonia. The mechanism of action of BoNT at the neuromuscular junction is well understood, however, aside from reports focused on myosin heavy chain isoform abundance, there is a paucity of data addressing the effects of therapeutic BoNT injection on the TA muscle proteome. In this study, 12 adult Sprague Dawley rats underwent unilateral TA muscle BoNT serotype A injection followed by tissue harvest at 72 hrs, 7 days, 14 days, and 56 days post-injection. Three additional rats were reserved as controls. Proteomic analysis was performed using 2D SDS-PAGE followed by MALDI-MS. Vocal fold movement was significantly reduced by 72 hrs, with complete return of function by 56 days. Twenty-five protein spots demonstrated significant protein abundance changes following BoNT injection, and were associated with alterations in energy metabolism, muscle contractile function, cellular stress response, transcription, translation, and cell proliferation. A number of protein abundance changes persisted beyond the return of gross physiologic TA function. These findings represent the first report of BoNT induced changes in any skeletal muscle proteome, and reinforce the utility of applying proteomic tools to the study of system-wide biological processes in normal and perturbed TA muscle function.

Keywords

Thyroarytenoid muscle; botulinum toxin; proteome; two-dimensional gel electrophoresis; mass spectrometry

1. Introduction

Botulinum neurotoxin (BoNT) is a potent agent that induces muscle paresis or paralysis by entering neurons and disrupting acetylcholine (ACh) release into the neuromuscular junction [1,2]. Seven BoNT serotypes are known to exist (A-G), all of which are produced by strains of the bacterium *Clostridium botulinum*. BoNT causes the paralytic syndrome botulism, but also holds therapeutic application in the treatment of dystonias [3–6], spasticity [7,8], facial rhytides [9], axillary hyperhidrosis [10,11], and some pain syndromes [12,13].

Correspondence: Nathan V. Welham, Ph.D., K4/723 CSC, 600 Highland Avenue, Madison WI, 53792, USA. Email: E-mail: welham@surgery.wisc.edu, Fax: 608-263-7652.

BoNT injection into one or several intrinsic laryngeal muscles is the most commonly performed medical intervention for spasmodic dysphonia; a debilitating voice disorder characterized by involuntary phonatory interruptions and impaired voice quality. This form of treatment is successful in alleviating voice symptoms temporarily [3]; however, as a peripheral (and symptom) based treatment for a central nervous system disorder, it does not provide a cure. Therefore, BoNT therapy must be readministered periodically. The mechanism of action of BoNT in the neuron and its effect on ACh release at the neuromuscular junction are generally understood [2], however relatively little is known about the effects of therapeutic BoNT injection on the cellular and molecular properties of the target muscle itself. This is an important avenue of investigation, as any such effects may hold implications for the variability in therapeutic response observed both across and within patients, the duration of therapeutic benefit and nature of relapse following a single injection, and the long-term consequences of repeated injections.

Previous work in rat intrinsic laryngeal muscle has demonstrated increased acute and chronic cellular mitotic activity following BoNT injection [14], suggesting that BoNT induces a proliferative response in muscle tissue; however the precise nature and significance of this response, including the cell types involved (i.e., satellite and/or fibroblast) and their associated transcriptional/translational behaviors, is unclear. Decreased muscle fiber diameter [15,16], endomysial fibrosis [15], and changes in myosin heavy chain (MyHC) isoform distribution [15,17] have also been reported. Inagi et al. [17], in discussing the MyHC isoform alterations observed in their study, noted discrepancy between their findings and those reported in the literature for denervation by recurrent laryngeal nerve resection and suggested that their findings may have been due to chemodenervation induced by BoNT activity in the neuron, and/or the direct activity of BoNT on the muscle itself.

The observation that BoNT induced intrinsic laryngeal muscle changes may be distinct from those observed following other modes of denervation highlights the importance of studying this clinically relevant process. Proteomic analysis of rat thyroarytenoid (TA) muscle following recurrent laryngeal nerve resection has demonstrated system-wide changes in protein abundance [18], however the degree of correspondence between these changes and those associated with BoNT treatment is unknown. The goal of this study was to characterize the complex array of protein abundance changes in the rat thyroarytenoid (TA) muscle at a series of time points following BoNT chemodenervation using 2D SDS-PAGE and MALDI-MS. We selected the TA muscle over other intrinsic laryngeal muscles as it is the primary muscle of the vocal fold, holds highly specialized functions for voice and swallowing, has a unique MyHC profile, and is a common target for therapeutic BoNT injection.

2. Materials and Methods

2.1 Experimental animals

Fifteen nine-month-old male Fisher 344/Brown Norway Cross inbred rats were used in this study. The rats had a mean body weight of 436 g (*SD* = 45 g). Twelve rats underwent laryngoscopy and BoNT injection. Euthanasia and muscle harvest were performed at four time points (3 rats per time point): 72 hr, 7 days, 14 days, and 56 days post-injection. The initial and final time points were selected based on previous work demonstrating a robust chemodenervation effect by 72 hr post injection, with complete return of function by 56 days post injection [14,17,19]. Three rats, employed as controls, underwent laryngoscopy and immediate euthanasia followed by muscle harvest.

2.2 Laryngeal visualization and BoNT injection

Anesthesia was induced using 2–3% isoflurane gas delivered at 0.8–1.5 L/min and maintained using an intraperiotoneal injection of ketamine hydrochloride (70 mg/kg) and xylazine hydrochloride (5 mg/kg). Atropine sulfate (52 μg/kg) was administered in order to reduce salivary secretions and assist with laryngeal visualization.

Laryngeal visualization was performed using a custom laryngoscope [20] and operating platform [16,21] in addition to a 1.9 mm diameter 25° rigid endoscope (Richard Wolf, Vernon Hills, IL) coupled to a halogen light source, display monitor and digital video camera (Sony DCR-PC100, Tokyo, Japan). Vocal fold opening and closure during respiration were recorded immediately prior to BoNT injection, at 72 hr post-injection and immediately prior to euthanasia and muscle harvest. These data were also collected from the control animals. A previous report documented that vocal fold movement during respiration is unaffected by the anesthesia cocktail used here [20].

Commercial BoNT serotype A (BoNT/A) (Botox®, Allergan Pharmaceuticals, Irvine, CA) was reconstituted in 0.9% saline and injected at a concentration of 0.01 U in 0.4 μL, using a 5 μL syringe with a 50 mm, 26-gauge needle. Injections were unilateral, and made into the TA muscle under endoscopic guidance (Figure 1).

Measurements of vocal fold movement during respiration were employed to confirm BoNT effect, as illustrated in Figure 1. All measurements were made using Photoshop 7.0 (Adobe Systems, San Jose, CA). Still frames were selected representing maximum vocal fold opening (during inhalation) and closure (during exhalation). A reference line was constructed between points at the anterior (A) and posterior (P) commissures. Two additional lines were drawn between P and points on the vocal fold medial edge at the right (R) and left (L) vocal processes. Angles APL and APR were measured and compared across the maximum opening and closure frames. Vocal fold movement angle was calculated by subtracting the maximum vocal fold closure angle from the maximum vocal fold opening angle, on a given side. Sample identity was masked and all measurements were performed in random sequence to control for any order effect. Inter- and intra-measurer agreement data were collected for 50% of all measurements.

2.3 Laryngeal harvest and dissection procedures

Euthanasia was performed via intracardiac injection of Beuthanasia (0.22 mL/kg). The larynx was harvested en bloc, and dissected using a surgical microscope and microsurgical instruments. The larynx was separated along the midline, allowing separate treatment of the left and right sides. A longitudinal incision was made in the subglottis, and the mucosa was undermined as far as the supraglottis to expose the TA muscle. The entire muscle body (muscularis and vocalis) was then harvested by dissection, proceeding anteriorly from the lateral base of the arytenoid cartilage to the thyroid cartilage. Following each dissection, the remaining hemilarynx was inspected to ensure that the non-TA intrinsic laryngeal muscles remained intact and undisturbed. The time duration from euthanasia to completion of dissection was approximately 10 min in all cases.

2.4 Sample preparation

Muscle samples were placed in 25 μL osmotic lysis buffer (0.3% SDS, 10 mM Tris; pH 7.4) containing 10% nuclease inhibitor (500 μg/mL RNase, 1 mg/mL DNase, 50 mM $MgCl_2$, 100 mM Tris; pH 7.0) and 1% protease inhibitor (20 mM AEBSF, 1 mg/mL leupeptin, 360 μg/mL E-64, 500 mM EDTA, 560 μg/mL benzamidine) solutions. Tissue homogenization was performed on ice using an ultrasonic homogenizer (BioLogics Model 300V/T, Manassas, VA) for 6 min at 40% power with a micro tip. After the addition of 25 μL boiling buffer (5% SDS, 10% glycerol, 60 mM Tris; pH 6.8), the samples were placed in a boiling water bath for 30

min to facilitate dissolution, cooled on ice, and then centrifuged to pellet solids. The samples were then frozen and stored at −80° C in preparation for total protein quantitation and electrophoresis.

Total protein quantitation was performed spectrophotometrically using the bicinchoninic acid method [22] and kit produced by Pierce Biotechnologies (Rockford, IL). BSA was employed as a standard and absorbance at 562 nm was measured using the Smart Spec 3000 spectrophotometer (BioRad Laboratories, Hercules, CA). Each assay was replicated, and final results were averaged. Mean final measurements of total protein ranged from 50–350 μg across all samples.

2.5 Electrophoresis

2D SDS-PAGE was performed using the carrier ampholine isoelectric focusing method [23]. Total protein sample load was 50 μg for gels intended for silver staining and image analysis (one per animal, three per experimental time point), and 225 μg for a series of replicate gels (one per experimental time point) intended for Coomassie blue staining and spot excision. Isoelectric focusing was performed in glass tubes (2.0 mm inner diameter) using 2.0% pH 3.5–10 ampholines (Amersham Pharmacia Biotech, Piscataway, NJ) for 9600 Vh.

After equilibrium for 10 min in buffer (10% glycerol, 50 mM dithiothreitol, 2.3% SDS and 0.0625 M Tris; pH 6.8), each tube gel was sealed to the top of a stacking gel above a 7.5 mm thick 10% acrylamide slab gel. SDS slab gel electrophoresis was performed for approximately 4 hrs using 12.5 mA/gel. Six proteins (Sigma, St. Louis, MO) were added to the agarose used to seal the tube gel to the slab gel, as MW standards: Myosin (220 kDa), phosphorylase A (94 kDa), catalase (60 kDa), actin (43 kDa), carbonic anhydrase (29 kDa) and lysozyme (14 kDa). These standards appear along the basic edge of each gel. The gels were either silver [24] or Coomassie blue stained. Gels were dried between cellophane paper.

2.6 Gel image analyses

Gels were scanned using an Agfa Arcus II flatbed scanner (Agfa, Mortsel, Belgium) in transparent mode, at 200 dpi resolution and 24-bit image depth. Image analysis was performed using Melanie 4.02 (GeneBio, Geneva, Switzerland) [25–27]; and a previously reported analysis protocol [28]. Briefly, automatic spot detection was performed and then refined by adjustment of the primary detection parameters (number of smoothing passes, saliency of the spot feature, minimum pixel area) in conjunction with visual inspection. Final parameter values, judged as providing optimal detection across all 15 gels, were 2 smoothing passes, a 3.5 saliency value, and 18 pixels minimum area. Following automatic detection, matching was performed for all silver-stained gels within their respective experimental groups (control, 72 hr, 7 days, 14 days, 56 days post-injection) and across the entire population of 15 silver-stained gels. The gel with the greatest number of protein spots in each experimental group was selected as the reference gel. Six widely distributed and visually salient proteins were selected as starting landmarks for the matching algorithm.

Spot-by-spot visual inspection and manual correction of detection and matching errors were performed by an expert gel analyst using each gel image, its 3-dimensional representation, and an intensity variation profile based on its entire 24-bit image depth. Sample identity was masked. All ratings were performed in random sequence to control for any order effect.

Synthetic master gels were constructed representing each of the 5 experimental groups. The gel with the greatest number of protein spots in each experimental group was again selected as the reference gel. Spots added to each synthetic gel were exclusive to those consistently

detected and matched across all 3 constituent gels. Automatic spot matching, visual inspection, and manual correction were performed using the synthetic control gel as the reference.

Number of spots detected in each gel, and number and percentage of spots matched within the 5 experimental groups, 5 synthetic gels, and across all 15 gels were measured. Normalized spot volume was calculated using standard software algorithms. Estimated MW values for identified spots were determined by logarithmic interpolation and extrapolation of values for the MW standards present along the basic edge of each gel. Estimated p*I* values were determined by linear interpolation and extrapolation of surface pH measurements taken from four blank isoelectric focusing tube gels.

Qualitative observations of consistent protein spot presence/absence across experimental groups were noted during the visual inspection and manual correction of spot detection and matching. The purpose of this additional visual-perceptual analysis was to detect any potentially interesting spots that, due to their consistent absence in at least one experimental condition, were not detected by the spot matching algorithm and therefore not included in the quantitative analysis. Criteria for spot observations of potential importance were defined as follows: a) present in all 3 control gels and absent in all 3 gels in at least one other experimental group; or b) absent from all 3 control gels and present in all 3 gels in at least one other experimental group.

2.7 Protein spot identification

Spots of interest were manually excised from the Coomassie blue stained gels, transferred to clean tubes and rehydrated in Milli-Q water (Millipore, Bedford, MA). Spots were prepared for digestion by washing twice with 100 μL 0.05 M Tris, pH 8.5/30% acetonitrile for 20 min with shaking, then with 100% acetonitrile for 1–2 min, before drying for 30 min in a Speed-Vac concentrator.

Samples were digested using 0.06 μg modified trypsin (sequencing grade, Roche Molecular Biochemicals, Indianapolis, IN) in 13–15 μL 0.025 M Tris, pH 8.5 and then incubated at 32° C overnight. Peptides were extracted using 2× 50 μL 50% acetonitrile/2% TFA and the combined extracts were dried and resuspended in 3 μL matrix solution consisting of 10 mg/mL 4-hydroxy-α-cyanocinnamic acid in 50% acetonitrile/0.1% TFA and containing two internal standards, angiotensin and ACTH 7–38 peptide. Following resuspension, 0.5 μL of each sample was spotted onto a MALDI plate and, once dry, washed twice with Milli-Q water. MALDI-MS was performed on the digested samples using a Voyager DE Pro mass spectrometer (Applied Biosystems, Foster City, CA) in the linear mode.

Peptide mass data were analyzed using ProFound (http://prowl.rockefeller.edu) and the MS-Fit module of the ProteinProspector program (http://prospector.ucsf.edu, version 4.0.8), and the NCBI and/or GenPept protein databases. Mass range was set at 900–5000 Da and mass error tolerance was set at 0.5 Da. Minimum fragment length was 5 peptides. A maximum of one missed cleavage was allowed. Acrylamide modified cysteine residues were allowed.

2.8 Statistical analyses

Vocal fold movement angle data were analyzed using Wilcoxon rank sum tests. Inter- and intra-measurer agreement data were analyzed using the Bland-Altman procedure with limits of agreement set at 95% [29]. Percentage of spots matched across gels was calculated using a previously reported algorithm [27]. Statistical comparisons were performed for each group of matched spots in the standard (i.e., non-synthetic) gels using a series of one-way ANOVAs, with experimental group as a fixed effect. Post-hoc pairwise comparisons of significant main effects were then performed for each post-injection experimental group against the control

group. A parallel analysis using the synthetic gel set was conducted by calculating percentage change in normalized spot volume for each post-injection gel compared with the control gel. An α-level of 0.01 was employed for all statistical testing.

3. Results

3.1 Vocal fold movement data

Vocal fold movement data are summarized in Figure 2. Decreased movement of the injected vocal fold was consistently observed for all rats (excluding controls) at the 72 hr time point ($p < 0.0001$). Movement data collected by time point immediately prior to TA muscle harvest revealed a general trend of reduced vocal fold movement by 72 hr, maintenance of this effect at 7 days, initiation of remission by 14 days, and a return to approximate pre-injection movement by 56 days post-injection. No statistically significant differences were observed between any of the post-injection experimental groups and the control group.

Bland-Altman analysis of inter- and intra-measurer agreement data revealed −0.98° bias (95% CI, −1.91° to −0.04°), −6.54° lower limit of agreement, and 4.59° upper limit of agreement for the inter-measurer comparison, and −0.11° bias (95% CI, −0.75° to 0.53°), −3.93° lower limit of agreement, and 3.71° upper limit of agreement for the intra-measurer comparison.

3.2 Protein spot detection and matching

The number of spots matched across all 3 gels in a single experimental group was 557 (90.7%) in the control group and ranged from 389–481 (65.0–79.6%) in the post-injection groups. The number of spots matched between the control group and each post-injection experimental group ranged from 307–343 (49.3–56.3%). A total of 199 spots (33.2%) were matched across all gels and experimental groups.

3.3 Protein spot quantitation

Twenty protein spots (Figure 3: Spots 1–20) demonstrated statistically significant differences in normalized spot volume (increased volume in 10 cases; decreased volume in 10 cases) across experimental groups (Figure 4). The percentage change in normalized volume that reached significance ranged from 28.9–690.7%. Patterns of normalized volume change were different across the various post-injection experimental groups when compared to control; however, the direction of change was consistent in the majority of cases (17 of 20 spot groups).

It is important to highlight that statistical testing identified a number of proteins with spot abundance changes below the 2 or 3-fold (100 or 200% increase) threshold commonly employed in 2D gel image analysis. Because of this, data for proteins with modest but statistically significant spot abundance changes were interpreted judiciously.

Five protein spots (Figure 3: Spots 21–25) were identified as potentially biologically significant during qualitative gel analysis. Spots 21 and 22 were present in all 3 control gels and absent in all 12 post-injection gels. Spots 23–25 were present in all 12 post-injection gels and absent in all 3 control gels. Exemplar gel images representing spot 23 (MW, 33.8 kDa; p*I*, 6.20) are presented in Figure 5.

3.4 Protein identification

MALDI-MS and database searching results are summarized in Table 1. Protein species were successfully identified in 20 of the 25 samples. Four spots demonstrated multiple protein species.

4. Discussion

This study examined changes in the rat TA muscle proteome following chemodenervation by BoNT/A injection. Normal TA muscle was compared with TA muscle at four post-injection time points (72 hr, 7 days, 14 days, 56 days). Vocal fold movement during respiration was measured to confirm gross physiologic BoNT/A effect. Both quantitative and qualitative analyses revealed significant changes in the rat TA muscle proteome following BoNT/A injection. The quantitative analyses revealed significant changes in abundance for 20 proteins identified and matched across experimental groups. The qualitative analysis highlighted three protein spots present exclusively in the post-injection experimental gels, and two protein spots present exclusively in the control gels. Further, the quantitative analyses revealed significant changes in individual protein abundance levels at different post-injection time points, whereas the qualitative analysis revealed proteomic variations that appeared reliably characteristic of either the control or post-injection (irrespective of time point) conditions. This suggests that while some proteins hold transient functions within the multiplex of biological processes involved in post-injection muscle alteration, others hold relatively stable functions that are established by 72 hr post-injection and sustained for at least 56 days.

4.1 Functional protein categories

Evaluation of those proteins identified by MADLI-MS and database searching revealed five major functional categories: Energy metabolism, contractile function, stress response, transcription/translation/cell proliferation, and miscellaneous. Protein spots within each category were characterized by both increased and decreased abundance, indicating dynamic ongoing biologic processes across each functional domain.

4.1.1 Energy metabolism—Five proteins identified in this study are associated with energy metabolism: Adenosine triphosphate (ATP) synthase (α, β and D chains), β-enolase, creatine kinase, glyceraldehyde-3-phosphate dehydrogenase (GAPDH), and aldolase A. ATP synthase functions to produce ATP from adenosine diphosphate, providing a critical energy source for cell function [30]. ATP synthase α chain, a regulatory subunit, demonstrated greater spot abundance at 72 hr, 7 days, and 56 days post-injection. Both the β-chain (catalytic subunit) and D chain (unknown function) had reduced spot abundance at 14 days. This contrasts with previous reports of ATP synthase upregulation in rat TA and soleus muscles following denervation and hindlimb suspension [18,31–32].

β-enolase, identified in two spot locations, demonstrated reduced spot abundance in both locations at 14 and 56 days. This muscle specific glycolytic enzyme holds important roles in striated muscle development and regeneration, and is more abundant in fast-twitch muscles, such as the TA, than slow-twitch muscles [33]. Previous reports have observed downregulation of β-enolase in aged rat gastrocnemius, denervated rabbit gastrocnemius and denervated rat TA muscle [18,33–34]. Creatine kinase, a major energy transduction enzyme and consumer of ATP, had reduced spot abundance at all post-injection time points, although it is important to note that a second protein, troponin T, was also identified in the same spot sample. Creatine kinase downregulation has been identified in aged and denervated rat gastrocnemius muscle [34–36]; however upregulation of this protein has been reported for denervated rat TA muscle [18].

Two additional glycolytic enzymes, GAPDH and aldolase A, were identified in spot locations that were characteristic of all 12 post-injection gels. These proteins are ubiquitous in normal skeletal muscle [37] and their gel presentation here suggests the possibility of a targeted degradation process, such as due to oxidative stress (consistent with the concomitant changes in superoxide dismutase and peroxiredoxin-3 discussed in Section 4.1.3.), or a BoNT/A

induced PTM. Changes in GAPDH abundance across multiple spot locations have also been reported in the aged rat gastrocnemius proteome [34].

4.1.2. Contractile function—Four identified proteins hold important muscle contractile functions: α-actin, tropomyosin β-chain, troponin T, and MyHC IIb. α-actin, identified in two spot locations, was consistently found in the same spot sample as other protein species at a significant distance from its theoretical MW/p*I*. Abundance was significantly increased at 72 hr, 7 days and 56 days post injection, which contrasts with previous reports of decreased α-actin abundance in denervated and aged rat skeletal muscle [32,34–35].

Tropomyosin β-chain, which regulates access to myosin binding sites on the actin filament, demonstrated reduced spot abundance at 14 days post-injection, before recovering by 56 days post-injection. Previous proteomic studies have confirmed the downregulation and subsequent recovery of tropomyosin β-chain in denervated and then reinnervated rat gastrocnemius muscle [35], in addition to the downregulation of tropomyosin α-chain in aged rat gastrocnemius muscle [36]. Troponin T, which binds to tropomyosin in the thin filament regulatory complex, is reportedly downregulated in rat soleus muscle following denervation and hindlimb suspension [31–32]. In this study, troponin T demonstrated increased abundance at all post-injection time points in one spot location, and reduced abundance at all post-injection time points in a second spot location. This finding is similar to that reported by Piec et al. who identified both up and downregulation of three different Troponin T isoforms across four spot locations in the aged rat gastrocnemius proteome [34].

MyHC IIb demonstrated increased abundance at 72 hr, 7 days and 56 days in one spot location (shared with vitamin D binding protein [VDBP] and α-actin), and was present in a second spot location characteristic of all 12 post-injection gels. Upregulation of MyHC IIb for at least 56 days following BoNT/A injection in the rat TA was reported by Inagi et al., alongside concomitant upregulation of MyHC IIx and downregulation of IIL [17]. These findings suggest a general shift from superfast to fast MyHC isoform predominance following BoNT/A injection, and contrast with other reports of decreased MyHC IIb abundance following surgical denervation [35].

4.1.3 Stress response—Three proteins identified in this study indicate the presence of a cellular stress response following BoNT/A injection. Superoxide dismutase, an antioxidant enzyme that catalyzes superoxide into oxygen and hydrogen peroxide [38], demonstrated increased spot abundance 7 days post-injection; whereas peroxiredoxin-3, another antioxidant enzyme that functions to catalyze peroxides [39], demonstrated reduced spot abundance at 14 days post-injection. Sixty kDa heat shock protein (Hsp60), identified in the same spot location as α-actin, showed increased spot abundance at 72 hr and 7 days post-injection. Previous reports in denervated and aged skeletal muscle have documented elevated expression of other heat shock proteins, but not specifically Hsp60 [32,34].

4.1.4 Transcription, Translation, Cell Proliferation—Two identified proteins hold functions related to gene transcription, protein translation and cell proliferation. Prohibitin, which demonstrated increased spot abundance at all time points following BoNT/A injection, functions to inhibit DNA synthesis and cell proliferation, and also appears to play a role in transcriptional regulation within the cell [40]. Tufm protein, which showed reduced spot abundance at 72 hr, 7 days and 14 days post-injection, plays a key role in protein elongation as part of translation [41]. Neither protein has been identified in previous proteomic analyses of skeletal muscle dysfunction.

4.1.5 Miscellaneous—Three additional proteins with a significant change in spot abundance following BoNT/A injection were VDBP, phosphatidylethanolamine-binding protein (PEBP)

1, and protein disulfide isomerase. VDBP is the primary plasma carrier protein for vitamin D, but also binds monomeric actin, assists in fatty acid transport and plays a role in macrophage activation [42]. VDBP, identified in the same spot location as two other proteins, demonstrated increased spot abundance at 72 hr, 7 days and 56 days post-injection. This finding is consistent with a previous report of elevated VDBP in the aged rat gastrocnemius proteome [34]. PEBP 1, which demonstrated increased spot abundance at 7 and 14 days post-injection, functions as a serine protease inhibitor, and binds ATP, opioids and the phospholipid phosphatidylethanolamine. Protein disulfide isomerase, which also demonstrated increased spot abundance at 72 hr and 14 days, is an enzyme which catalyzes the formation and cleavage of disulfide bonds during protein folding [43]. Upregulation of protein disulfide isomerase has also been reported in the aged rat gastrocnemius proteome [34].

4.2 Persistence of proteomic changes

The persistence of proteomic changes following the resolution of gross vocal fold movement to pre-injection levels suggests the possibility of long-term (beyond 56 days for the dose employed in this experiment) or even permanent muscle protein changes as a result of BoNT/A injection. Such changes could be adaptive, reflecting ongoing repair, recovery, and compensatory processes; maladaptive, resulting in subtle but significant functional impairment not evident in gross vocal fold movement; or sub-functional and clinically irrelevant. Although the mechanistic nature of these changes is uncertain, it is important to note that any extended alterations in the TA muscle proteome following BoNT/A injection could have implications for the long-term outcomes of patients who receive periodic therapeutic BoNT/A injections for the management of focal dystonias such as spasmodic dysphonia.

The wider literature contains varied reports concerning the presence of long-term muscle structure and function changes following BoNT/A exposure. In their series of studies investigating BoNT/A (0.07 U) in the rat TA muscle, Inagi et al. reported a return to baseline satellite cell mitotic activity by 28 days post-injection [14], a return to baseline vocal fold movement levels at 31.3 days and electromyographic interference pattern at 39.5 days post-injection [21], and a persistence of relative MyHC isoform changes (reduction in type IIL, increase in types IIb and IIx) at 56 days post-injection [17]. Hassan et al. [44], reporting on BoNT/A (~100 U) in the rat gastrocnemius muscle, noted full recovery of leg function by 10–12 weeks post-injection, a return to baseline muscle fiber diameter by 18 weeks post-injection, and a persistence of subtle ultrastructural abnormalities at 30 weeks post-injection.

While differences in target muscle and BoNT/A dose make the direct comparison of results across studies challenging, it appears that some muscle changes (i.e., muscle fiber diameter reduction, proteomic variations including MyHC isoform alterations, and various ultrastructural abnormalities) do persist beyond the return of gross physiologic function. While some of these changes are transient and represent late-stage repair or perhaps compensatory processes, others may be permanent. Determining whether the proteomic and ultrastructural muscle changes identified in this experiment and other reports are transient or permanent requires collecting additional long-term post-injection data.

4.3 Protein heterogeneity

Several manifestations of protein heterogeneity were observed in this study. A number of proteins, such as α-actin, β-enolase, MyHC IIb and GAPDH, were identified in multiple spot locations with different MW/p*I* values. Further, certain proteins, such as α-actin, creatine kinase and MyHC IIb, exhibited experimental MW/p*I* values that departed significantly from their theoretical values. These spot patterns are difficult to interpret without additional data; however, as discussed above, they could represent a targeted degradation process involving an oxidative stress response, alternative mRNA splicing and/or PTM. Determination of which

protein changes are due to genuine alterations in abundance and which are due to differential PTM could be assisted by additional analysis using PTM specific antibodies and/or MS. Phosphorylation, the most commonly observed protein PTM, has been reported for select proteins (including β-enolase and creatine kinase) in denervated rat TA muscle [18].

In four cases, multiple proteins migrated to the same gel coordinates and were identified within the same gel spot. The interpretation of changes in protein abundance is difficult to interpret in these cases, as the relative contribution of each protein species to an overall shift in normalized spot volume is uncertain. Because of this, the interpretation of significant abundance changes for proteins identified in spots 5, 11, 13 and 24 must be made with caution, and can only be confirmed by further analysis. This challenge may be resolved by emerging techniques such as isotype-coated affinity tag labeling, which offer promise in delineating and quantifying multiple proteins within a single spot [45].

4.4 Conclusions and Future Directions

This study is the first to report BoNT/A induced changes in any skeletal muscle proteome, and the second to document experimentally induced changes in the rat TA muscle proteome. The proteome-wide abundance changes observed here appear to reflect a series of coordinated functional processes involving alterations in energy metabolism, muscle contractile function, cellular stress response, transcription, translation, and cell proliferation. A number of protein abundance changes persisted beyond the return of gross physiologic TA function. Certain protein changes bore similarity to those documented in other skeletal muscle denervation and aging models; whereas other changes appeared novel. These findings reinforce the utility of applying proteomic tools to the study of system-wide biological processes in normal and perturbed TA muscle function.

Further research is needed to extend proteome mapping and individual protein species identification, for the TA and other muscles, tissues and cell types of significance to voice, speech and swallowing function. Studies should examine a complement of subcellular fractions and whole cell homogenates, in order to capture both high and low abundance proteins, assist with the gross assignment of these proteins to their native subcellular structures, and specifically probe for PTMs associated with various physiologic and disease states.

Acknowledgments

This study was supported by grants R01 DC004428 and R03 DC008884 from the National Institute on Deafness and Other Communication Disorders, grant R01 HL069970 from the National Heart, Lung, and Blood Institute, and the Robert Zeek Memorial Laryngeal and Voice Research Fund in the Division of Otolaryngology, Department of Surgery, University of Wisconsin School of Medicine and Public Health. The authors acknowledge laboratory services provided by Kendrick Laboratories, Madison WI, and the Protein Core Facility at Columbia University Medical Center, New York, NY. Statistical consultation was provided by Alejandro Muñoz del Río, Ph.D., and Glen Leverson, Ph.D., Department of Surgery, University of Wisconsin School of Medicine and Public Health.

This study was performed in accordance with the PHS Policy on Humane Care and Use of Laboratory Animals, the NIH *Guide for the Care and Use of Laboratory Animals*, and the Animal Welfare Act (7 U.S.C. et seq.); the animal use protocol was approved by the Institutional Animal Care and Use Committee (IACUC) of the University of Wisconsin-Madison.

Abbreviations

ACh, acetylcholine; ATP, adenosine triphosphate; BoNT, botulinum neurotoxin; GAPDH, glyceraldehyde-3-phosphate dehydrogenase; Hsp60, 60 kDa heat shock protein; MyHC, myosin heavy chain; PEBP, phosphatidylethanolamine-binding protein; TA, thyroarytenoid; VDBP, vitamin D binding protein..

References

1. Dressler D, Adib Saberi F. Botulinum toxin: Mechanisms of action. Eur Neurol 2005;53:3–9. [PubMed: 15650306]
2. Turton K, Chaddock JA, Acharya KR. Botulinum and tetanus neurotoxins: Structure, function and therapeutic utility. Trends Biochem Sci 2002;27:552–558. [PubMed: 12417130]
3. Boutsen F, Cannito MP, Taylor M, Bender B. Botox treatment in adductor spasmodic dysphonia: A meta-analysis. J Speech Lang Hear Res 2002;45:469–481. [PubMed: 12069000]
4. Costa J, Espirito-Santo C, Borges A, Ferreira J, et al. Botulinum toxin type B for cervical dystonia. Cochrane Database Syst Rev 2005:CD004315. [PubMed: 15674941]
5. Costa J, Espirito-Santo C, Borges A, Ferreira J, et al. Botulinum toxin type A therapy for blepharospasm. Cochrane Database Syst Rev 2005:CD004900. [PubMed: 15674969]
6. Truong D, Duane DD, Jankovic J, Singer C, et al. Efficacy and safety of botulinum type A toxin (Dysport) in cervical dystonia: Results of the first US randomized, double-blind, placebo-controlled study. Mov Disord 2005;20:783–791. [PubMed: 15736159]
7. El-Etribi MA, Salem ME, El-Shakankiry HM, El-Kahky AM, El-Mahboub SM. The effect of botulinum toxin type-A injection on spasticity, range of motion and gait patterns in children with spastic diplegic cerebral palsy: An Egyptian study. Int J Rehabil Res 2004;27:275–281. [PubMed: 15572990]
8. Brashear A, Gordon MF, Elovic E, Kassicieh VD, et al. Intramuscular injection of botulinum toxin for the treatment of wrist and finger spasticity after a stroke. N Engl J Med 2002;347:395–400. [PubMed: 12167681]
9. Yamauchi PS, Lowe NJ. Botulinum toxin types A and B: Comparison of efficacy, duration, and dose-ranging studies for the treatment of facial rhytides and hyperhidrosis. Clin Dermatol 2004;22:34–39. [PubMed: 15158543]
10. Fitzgerald E, Feeley TM, Tierney S. Current treatments for axillary hyperhidrosis. Surgeon 2004;2:311–314. [PubMed: 15712569]
11. Nelson L, Bachoo P, Holmes J. Botulinum toxin type B: A new therapy for axillary hyperhidrosis. Br J Plast Surg 2005;58:228–232. [PubMed: 15710119]
12. Kamanli A, Kaya A, Ardicoglu O, Ozgocmen S, et al. Comparison of lidocaine injection, botulinum toxin injection, and dry needling to trigger points in myofascial pain syndrome. Rheumatol Int 2005;25:604–611. [PubMed: 15372199]
13. Smuts JA, Schultz D, Barnard A. Mechanism of action of botulinum toxin type A in migraine prevention: A pilot study. Headache 2004;44:801–805. [PubMed: 15330827]
14. Inagi K, Connor NP, Schultz E, Ford CN, et al. Increased acute and chronic mitotic activity in rat laryngeal muscles after botulinum toxin injection. Laryngoscope 1998;108:1055–1061. [PubMed: 9665256]
15. Chhetri DK, Blumin JH, Vinters HV, Berke GS. Histology of nerves and muscles in adductor spasmodic dysphonia. Ann Otol Rhinol Laryngol 2003;112:334–341. [PubMed: 12731628]
16. Inagi K, Ford CN, Rodriquez AA, Schultz E, et al. Efficacy of repeated botulinum toxin injections as a function of timing. Ann Otol Rhinol Laryngol 1997;106:1012–1019. [PubMed: 9415596]
17. Inagi K, Connor NP, Schultz E, Ford CN, et al. Muscle fiber-type changes induced by botulinum toxin injection in the rat larynx. Otolaryngol Head Neck Surg 1999;120:876–883. [PubMed: 10352443]
18. Li ZB, Lehar M, Samlan R, Flint PW. Proteomic analysis of rat laryngeal muscle following denervation. Proteomics 2005;5:4764–4776. [PubMed: 16281258]
19. Inagi K, Connor NP, Ford CN, Schultz E, et al. Physiologic assessment of botulinum toxin effects in the rat larynx. Laryngoscope 1998;108:1048–1054. [PubMed: 9665255]
20. Suzuki T, Connor NP, Lee K, Leverson G, Ford CN. Laryngeal-respiratory kinematics are impaired in aged rats. Ann Otol Rhinol Laryngol 2002;111:684–689. [PubMed: 12184588]
21. Inagi K, Rodriquez AA, Ford CN, Heisey DM. Transoral electromyographic recordings in botulinum toxin-injected rat larynges. Ann Otol Rhinol Laryngol 1997;106:956–964. [PubMed: 9373087]
22. Smith PK, Krohn RI, Hermanson GT, Mallia AK, et al. Measurement of protein using bicinchoninic acid. Anal Biochem 1985;150:76–85. [PubMed: 3843705]

23. O'Farrell PH. High resolution two-dimensional electrophoresis of proteins. J Biol Chem 1975;250:4007–4021. [PubMed: 236308]
24. Oakley BR, Kirsch DR, Morris NR. A simplified ultrasensitive silver stain for detecting proteins in polyacrylamide gels. Anal Biochem 1980;105:361–363. [PubMed: 6161559]
25. Appel RD, Vargas JR, Palagi PM, Walther D, Hochstrasser DF. Melanie II-a third-generation software package for analysis of two-dimensional electrophoresis images: II. Algorithms. Electrophoresis 1997;18:2735–2748. [PubMed: 9504805]
26. Appel RD, Palagi PM, Walther D, Vargas JR, et al. Melanie II--a third-generation software package for analysis of two-dimensional electrophoresis images: I. Features and user interface. Electrophoresis 1997;18:2724–2734. [PubMed: 9504804]
27. Swiss Institute of Bioinformatics. Melanie: The 2-D gel analysis software. User manual for version 4.02. Geneva: Author; 2003.
28. Welham NV, Marriott G, Bless DM. Proteomic profiling of rat thyroarytenoid muscle. J Speech Lang Hear Res 2006;49:671–685. [PubMed: 16787904]
29. Bland JM, Altman DG. Statistical methods for assessing agreement between two methods of clinical measurement. Lancet 1986;327:307–310. [PubMed: 2868172]
30. Das AM. Regulation of the mitochondrial ATP-synthase in health and disease. Mol Genet Metab 2003;79:71–82. [PubMed: 12809636]
31. Isfort RJ, Wang F, Greis KD, Sun Y, et al. Proteomic analysis of rat soleus muscle undergoing hindlimb suspension-induced atrophy and reweighting hypertrophy. Proteomics 2002;2:543–550. [PubMed: 11987128]
32. Isfort RJ, Hinkle RT, Jones MB, Wang F, et al. Proteomic analysis of the atrophying rat soleus muscle following denervation. Electrophoresis 2000;21:2228–2234. [PubMed: 10892733]
33. Nozais M, Merkulova T, Keller A, Janmot C, et al. Denervation of rabbit gastrocnemius and soleus muscles: Effect on muscle-specific enolase. Eur J Biochem 1999;263:195–201. [PubMed: 10429204]
34. Piec I, Listrat A, Alliot J, Chambon C, et al. Differential proteome analysis of aging in rat skeletal muscle. FASEB J 2005;19:1143–1145. [PubMed: 15831715]
35. Sun H, Liu J, Ding F, Wang X, et al. Investigation of differentially expressed proteins in rat gastrocnemius muscle during denervation-reinnervation. J Muscle Res Cell Motil 2006;27:241–250. [PubMed: 16752196]
36. O'Connell K, Gannon J, Doran P, Ohlendieck K. Proteomic profiling reveals a severely perturbed protein expression pattern in aged skeletal muscle. Int J Mol Med 2007;20:145–153. [PubMed: 17611631]
37. Yan JX, Harry RA, Wait R, Welson SY, et al. Separation and identification of rat skeletal muscle proteins using two-dimensional gel electrophoresis and mass spectrometry. Proteomics 2001;1:424–434. [PubMed: 11680887]
38. Culotta VC, Yang M, O'Halloran TV. Activation of superoxide dismutases: Putting the metal to the pedal. Biochim Biophys Acta 2006;1763:747–758. [PubMed: 16828895]
39. Rhee SG, Chae HZ, Kim K. Peroxiredoxins: A historical overview and speculative preview of novel mechanisms and emerging concepts in cell signaling. Free Radic Biol Med 2005;38:1543–1552. [PubMed: 15917183]
40. Mishra S, Murphy LC, Murphy LJ. The Prohibitins: Emerging roles in diverse functions. J Cell Mol Med 2006;10:353–363. [PubMed: 16796804]
41. Parmeggiani A, Nissen P. Elongation factor Tu-targeted antibiotics: Four different structures, two mechanisms of action. FEBS Lett 2006;580:4576–4581. [PubMed: 16876786]
42. Speeckaert M, Huang G, Delanghe JR, Taes YE. Biological and clinical aspects of the vitamin D binding protein (Gc-globulin) and its polymorphism. Clin Chim Acta 2006;372:33–42. [PubMed: 16697362]
43. Nagradova N. Enzymes catalyzing protein folding and their cellular functions. Curr Protein Pept Sci 2007;8:273–282. [PubMed: 17584121]
44. Hassan SM, Jennekens FG, Veldman H. Botulinum toxin-induced myopathy in the rat. Brain 1995;118(Pt 2):533–545. [PubMed: 7735893]

45. Smolka M, Zhou H, Aebersold R. Quantitative protein profiling using two-dimensional gel electrophoresis, isotope-coded affinity tag labeling, and mass spectrometry. Mol Cell Proteomics 2002;1:19–29. [PubMed: 12096137]

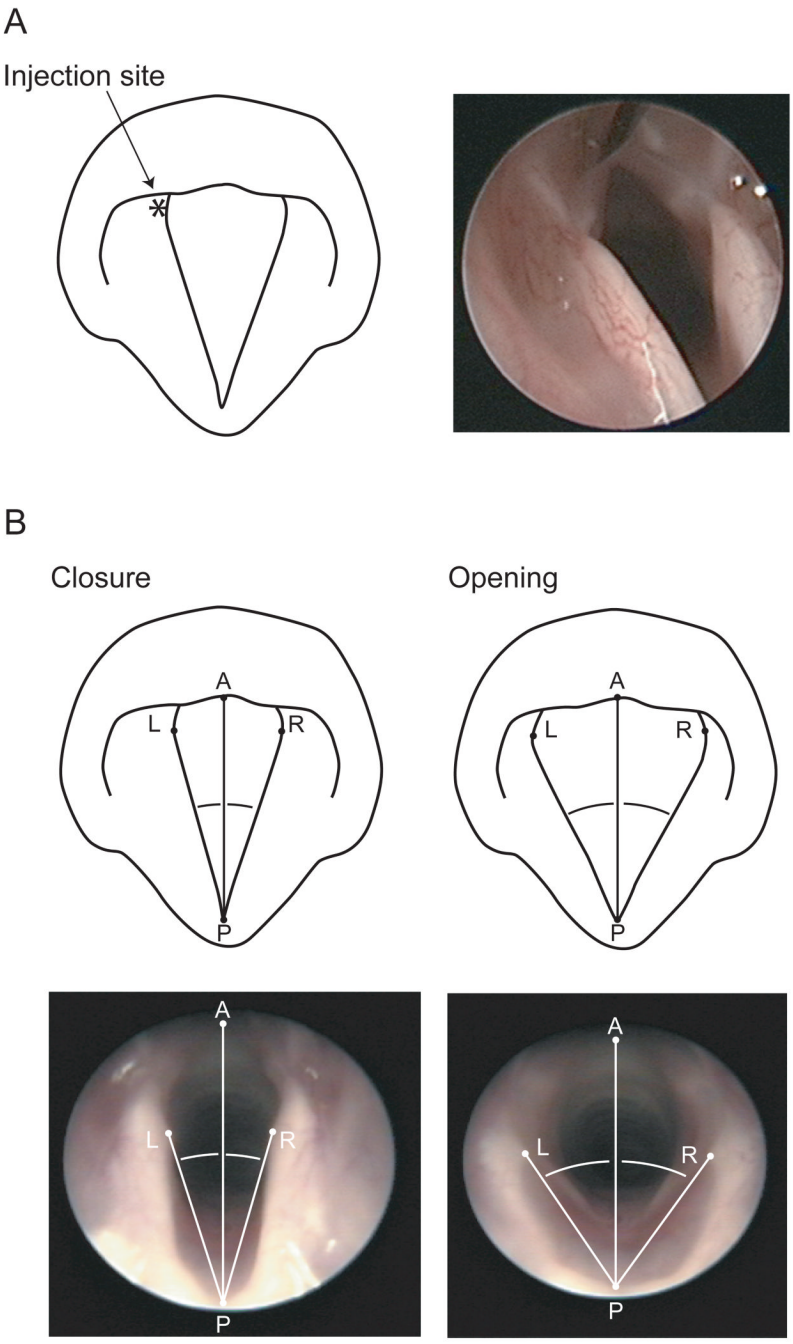

Figure 1.
Schematics and photographs illustrating (A) injection of BoNT/A into the left TA muscle using a 50 mm, 26-gauge needle and endoscopic guidance, and (B) measurement of maximum vocal fold opening (inspiratory) and closure (expiratory) angles during respiration. Vocal fold movement angle was calculated by subtracting the maximum vocal fold closure angle from the maximum vocal fold opening angle, on a given side. P, posterior commissure; A, anterior commissure; L, left vocal fold medial edge at left vocal process; R, right vocal fold medial edge at right vocal process.

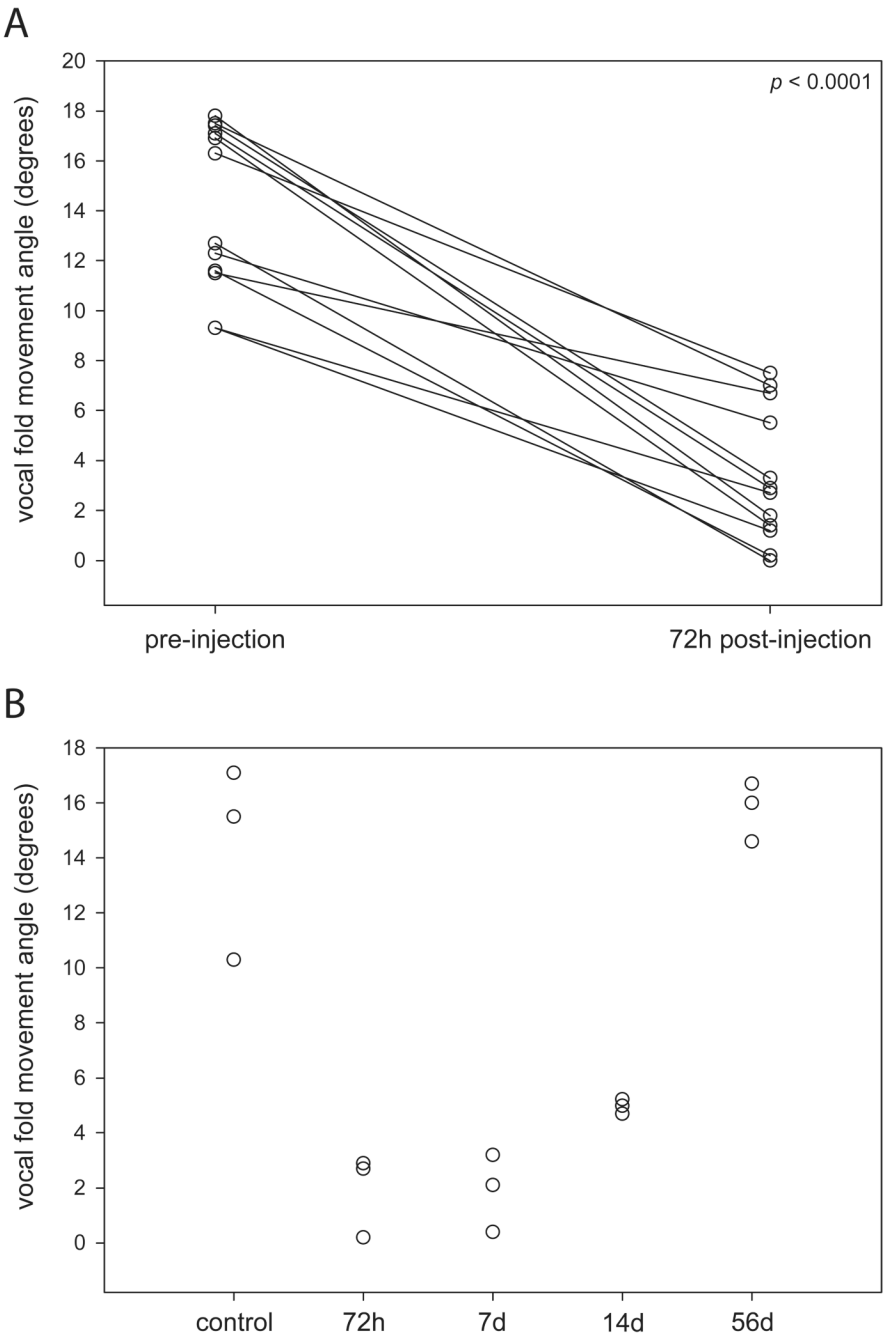

Figure 2.
Vocal fold movement angle data. (A) For all rats (excluding controls) immediately preceding and 72 hr following BotNT/A injection. (B) For all rats and all experimental groups, immediately prior to TA muscle harvest. Data represent the injected vocal fold only (except in the non-injected control group).

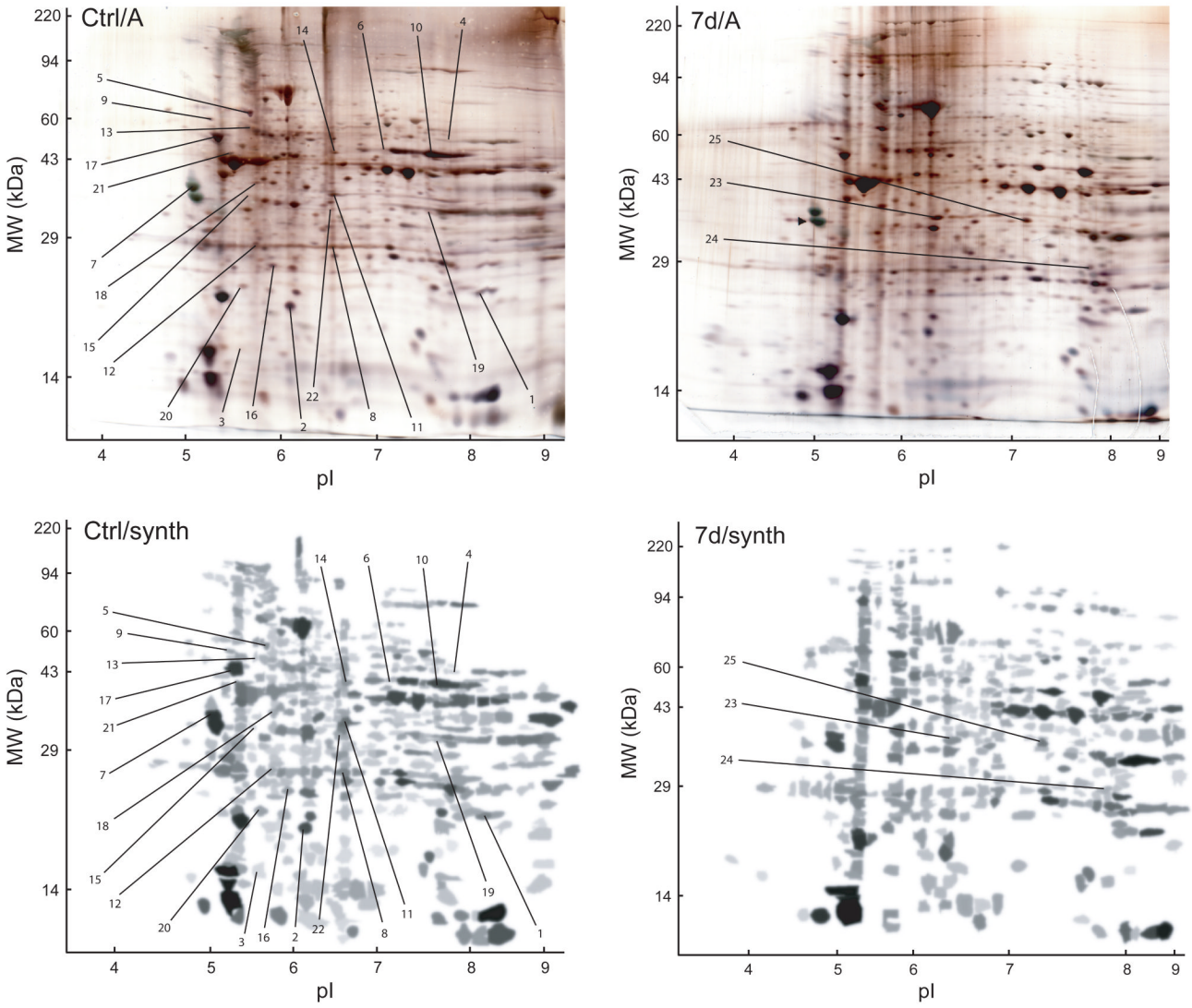

Figure 3.

Representative silver-stained SDS-polyacrylamide (Ctrl/A, 7d/A) and corresponding synthetic (Ctrl/synth, 7d/synth) gels with protein spots of interest labeled. Spots 1–20 demonstrated a statistically significant change in normalized volume across experimental conditions, spots 21 and 22 were present in all 3 control gels and absent in all 12 post-injection gels, and spots 23–25 were present in all 12 post-injection gels and absent in all 3 control gels.

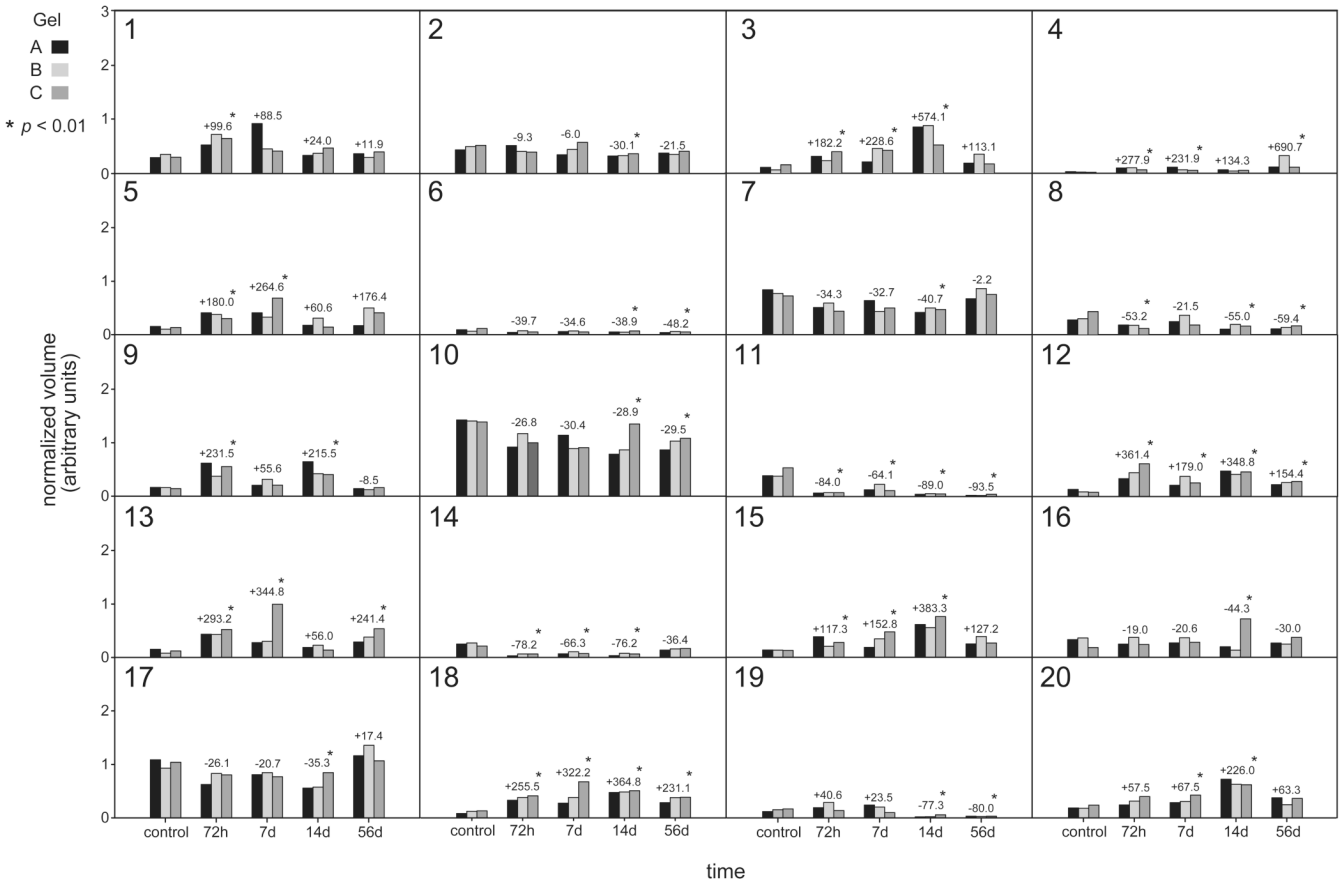

Figure 4.

Summary of statistically significant changes in protein expression level (normalized volume) for 20 protein spots in post-injection gels compared with control gels. Histogram bars represent normalized volume levels for spots in standard gels (3 per experimental group). Numeric annotations above the histogram bars represent percentage change in normalized volume from control, for spots in synthetic gels from each experimental group.

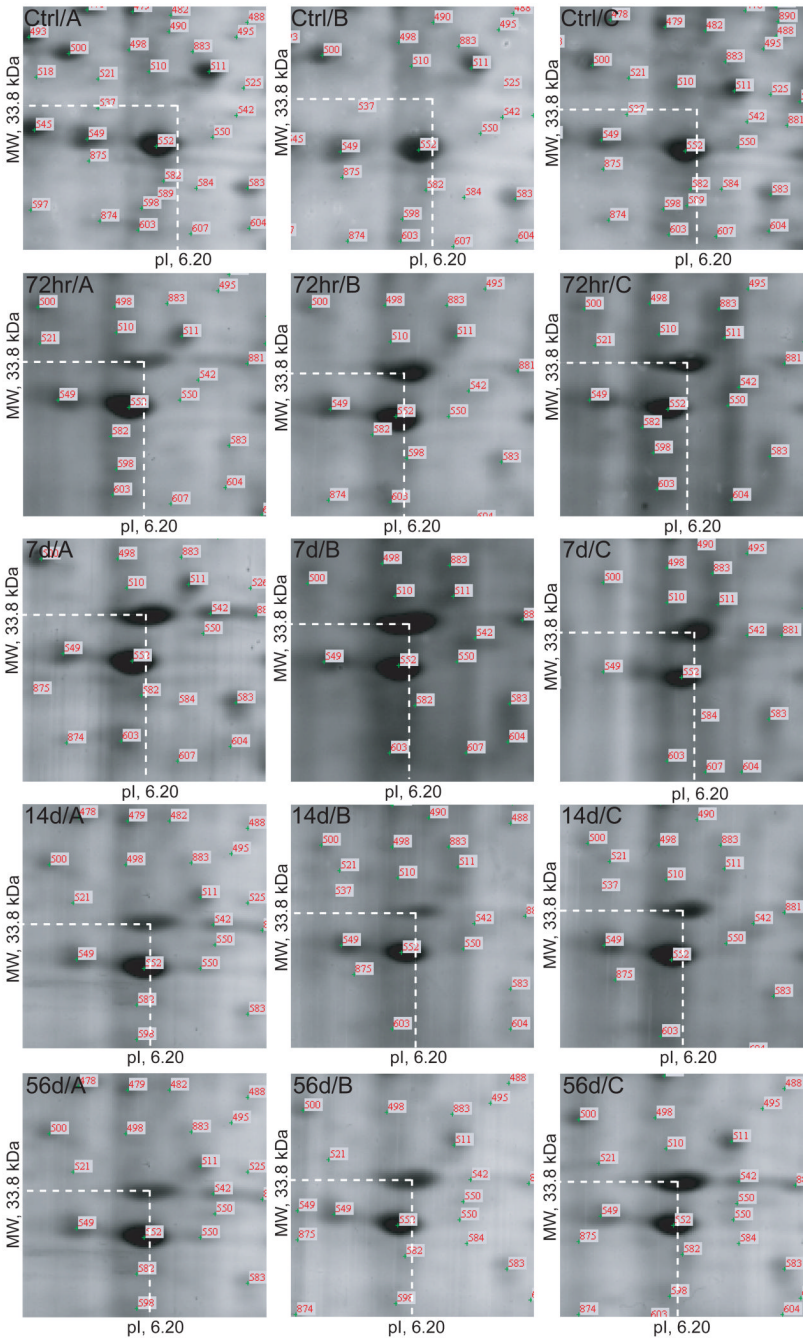

Figure 5.

Example of a protein spot (Spot 23, GAPDH: MW, 33.8 kDa; p*I*, 6.20) present in all 12 post-injection gels (representing all 4 post-injection time points) and absent in all 3 control gels.

Table 1

MALDI-MS identification of proteins demonstrating significant changes in expression in BoNT/A injected rat TA muscle compared with uninjected control.

Spot ID	Protein identified	Theoretical MW (kDa)/p*I*	Experimental MW (kDa)/p*I*	Sequence coverage (%)	Swiss-Prot/NCBI accession number
1	Superoxide dismutase [Mn]	22.3/7.94	23.9/8.43	74.2	P07895
2	ATP synthase D chain	18.6/6.21	22.6/6.11	61.9	P31399
3	Unidentified		18.6/5.53		
4	ATP synthase α-chain	55.3/8.28	53.3/7.79	49.4	P15999
5	a) Hsp60	57.9/5.35	65.9/5.60	62.0	P63039
	b) α-actin	41.8/5.23		26.7	P68035
6	β-enolase	46.9/6.81	48.6/7.03	51.2	P21550
7	Tropomyosin β-chain	32.8/4.66	35.2/5.07	56.3	P58775
8	MyHC IIb	61.0/5.40	28.8/6.53	28.8	GI:9581821
9	Protein disulfide isomerase	55.0/4.77	63.4/5.25	52.2	P04785
10	β-enolase	46.9/6.81	46.2/7.74	53.8	P21550
11	a) Troponin T, fast skeletal muscle	30.6/6.18	33.7/6.54	48.1	P09739
	b) Creatine kinase M-type	43.0/6.58		24.4	P07310
12	Prohibitin	29.8/5.57	28.9/5.65	62.5	P67779
13	a) MyHC IIb	61.0/5.40	60.0/5.67	58.3	GI:9581821
	b) VDBP	51.8/5.41		37.2	P04276
	c) α-actin	41.8/5.23		37.1	P68035
14	Tufm protein	47.2/7.60	47.4/6.55	42.5	GI:38173913
15	Unidentified		33.4/5.59		
16	Peroxiredoxin-3	21.6/5.81	26.5/6.16	70.8	Q9Z0V6
17	ATP synthase β-subuit	51.7/4.95	54.5/5.31	76.6	P10719
18	Troponin T, fast skeletal muscle	30.6/6.18	36.7/5.67	38.4	P09739
19	Unidentified		31.5/7.62		
20	PEBP 1	20.7/5.48	24.5/5.54	72.6	P31044
21	Unidentified		46.4/5.44		
22	Unidentified		31.8/6.53		
23	GAPDH	35.7/8.18	33.8/6.20	50.3	P04797
24	a) GAPDH	35.7/8.18	29.3/7.75	26.2	P04797

Spot ID	Protein identified	Theoretical MW (kDa)/p*I*	Experimental MW (kDa)/p*I*	Sequence coverage (%)	Swiss-Prot/NCBI accession number
	b) *Posssible:* Aldolase A	39.2/8.40		22.3	P05065
25	MyHC IIb	61.0/5.40	32.7/7.10	34.8	GI:9581821